Chinese Chemical Letters 34 (2023) 108030

Contents lists available at ScienceDirect

Chinese Chemical Letters

journal homepage: www.elsevier.com/locate/cclet

Quick fabrication of evenly porous PbO_2 through potential linear increase electrodeposition

Hua Guo[a,b], Wenyu Hu[a], Zekun Zhang[a], Duowen Yang[a], Siyuan Guo[a], Xiaosheng Jing[a], Hao Xu[a,b,*], Wei Yan[a,b]

[a] Department of Environmental Science and Engineering, Xi'an Jiaotong University, Xi'an 710049, China
[b] Research Institute of Xi'an Jiaotong University, Hangzhou 311200, China

ARTICLE INFO

Article history:
Received 8 September 2022
Revised 14 November 2022
Accepted 28 November 2022
Available online 30 November 2022

Keywords:
Lead dioxide
Bubble template
Porous electrode
Adsorption electrochemical porosity

ABSTRACT

Anodic oxidation electrodeposition is the primary way to prepare lead dioxide anode. The regulation of the external circuit for the reaction is a unique advantage of electrocatalytic reaction, which can regulate crystallization and accelerate the reaction process. In this study, lead dioxide coatings with uniform pore size distribution were quickly prepared on three different substrates by potential linear increase electrodeposition (PLIED). Morphology and structure analysis shows that the prepared electrodes have uniform porous morphology, and Ti/SnO_2/PLIED has the smallest grain size. Three electrodes all display well degradation performance to azophloxine and diclofenac sodium. Ti/PLIED, and Ti/SnO_2/PLIED are appreciated for degrading organics with a simple structure in low concentrations. At the same time, Ti/SnO_2/PLIED is more suitable for complex organics in high concentrations. Electrochemical activity tests indicate the different mechanisms of the PLIED electrodes that build the other degradation performance. Three PLIED electrodes show excellent electrical and electrochemical stability during the cycle degradation process. The results provide a reference for the subsequent anodic oxidation electrodeposition research and the regulating effect of the external circuit on coating properties.

As a common electrocatalytic material with low cost and high electro-catalytical activity, PbO_2 is widely applied in electrocatalytic fields, such as a lead-acid battery and organic electro-oxidation [1,2]. In recent years, there have been lots of studies about the modification of PbO_2 anodes to improve its performance, including, but not limited to, ionic doping, particle composite, *etc.* [3,4]. As electro-deposition is the most common fabrication method of PbO_2, more attention should be paid to the effects of external circuit regulation on electrode modification, which is the unique advantage of electrochemical reaction [5]. According to previous studies about electro-deposition parameters, it has been found that the variation of electrodeposition parameters strongly influences the crystallization process, which in turn changes the structure and morphology of PbO_2 coating and further affects the electrode properties [6,7].

As the external circuit is the driving force of electro-deposition, keeping a high overpotential effective accelerates the fabrication process, simultaneously, oxygen evolution reaction (OER) under the high potential can provide an *in-situ* bubble template to produce porous coating [8,9]. However, electrodeposition in a constant high potential is self-limited. The electrodeposition mechanism of PbO_2 is shown in Eqs. 1–3 [10]. The water splitting is the initiation step, which is boosted by the high overpotential. Pb(II) is quickly exhausted by massive OH_{ads} and produces PbO_2. And then, OER substitutes Pb(II) oxidation reaction. The electrodeposition process is restricted. The coexistence of the porous and nonporous area on the PbO_2 electrode fabricated by the potentiostatic electrodeposition with high potential suggests the uneven polarization during the process (Fig. S1 in Supporting information).

$$H_2O \rightarrow OH_{ads} + H^+ + e^- \quad (1)$$

$$Pb^{2+} + OH_{ads} \rightarrow Pb(OH)^{2+} \quad (2)$$

$$Pb(OH)^{2+} + H_2O \rightarrow PbO_2 + 3H^+ + e^- \quad (3)$$

Moreover, the simultaneous OER throughout the deposition process will expose the substrate of the fabricated electrode, which is detrimental to the long-term stability. Hence, potential increasing may be an available way to match deepening polarization and realize PbO_2 rapid and controllable electro-deposition. Additionally,

* Corresponding author at: Department of Environmental Science and Engineering, Xi'an Jiaotong University, Xi'an 710049, China.
E-mail address: xuhao@xjtu.edu.cn (H. Xu).

https://doi.org/10.1016/j.cclet.2022.108030
1001-8417/

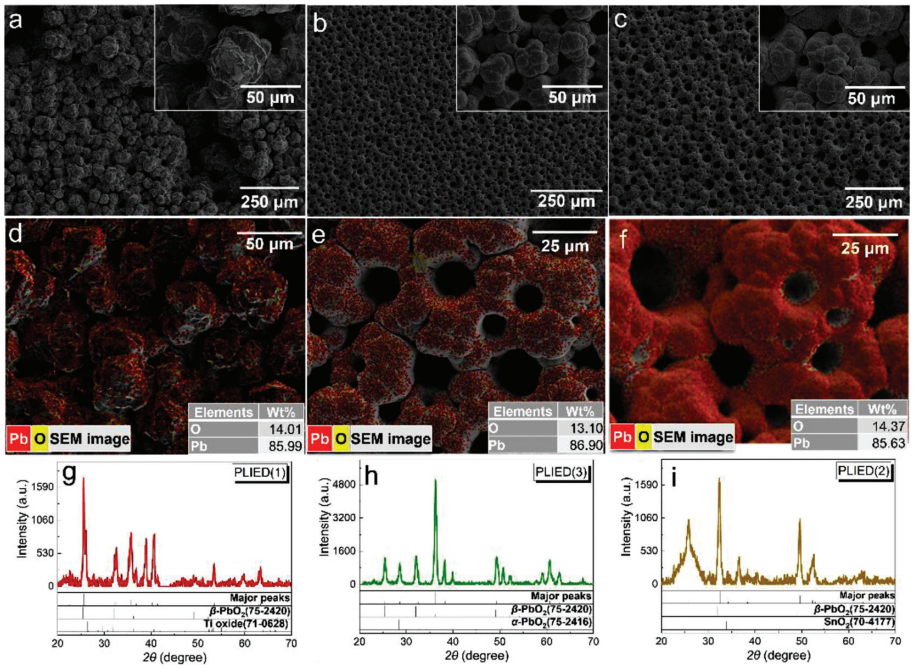

Fig. 1. SEM images (a–c), EDS mapping (d–f) and XRD patterns (g–i) of PLIED electrodes, (a,d,g) PLIED(1), (b, e, h) PLIED(2), and (c, f, i) PLIED(3).

a lower potential in the initial stage helps restrain oxygen bubbles and form a full-cover bottom. In addition, as a result of the concern about the stability of porous electrode, intermediate layer is a common choice. So, the influence of the intermediate layers to the effects of the potential manipulating needs to be considered too.

In this study, porous PbO_2 is quickly deposited on three substrates (with or without intermediate layers) through potential linear increase electrodeposition (PLIED) with an *in-situ* bubble template for the first time. The prepared PbO_2 electrodes are characterized by scanning electron microscopy (SEM), energy dispersive spectrum (EDS), and X-ray diffraction (XRD). The prepared PLIED electrodes served as the anodes in the electrochemical treatment of azophloxine (AR1) and diclofenac sodium (DCF) to evaluate the electrochemical degradation performance comprehensively. Electrochemical and hydroxyl radical productivities tests are conducted to estimate the electro-catalysis properties. Electrical and electrochemical stability also are characterized through cycle degradation tests.

Porous titanium plate (Baoji Yinggao Metal Material Ltd., China) with the dimension of $1\,cm^2 \times 1\,mm$ and filter fineness of 80 μm served as the substrate of PbO_2 electrode. The pre-treatment of the substrate and the fabrication of Sb–SnO_2 and -PbO_2 inter-layer were already elaborated in our previous works [11]. The electroplating bath consisted of 0.5 mol/L $Pb(NO_3)_2$, 0.2 mol/L $Cu(NO_3)_2$, and 0.01 mol/L NaF, in which the pH value was 2.0.

The PLIED processes were conducted by an electrochemical analyzer (CHI1140C, CH Instrument, Inc.) with an increasing rate of 50 mV/s in the range of 0–5 V at 65 °C. The titanium mesh with the same size acted as the counter electrodes. Furthermore, we marked the fabricated electrodes Ti/PLIED, Ti/SnO_2/PLIED, and Ti/SnO_2/-PbO_2/PLIED, as PLIED(1), PLIED(2) and PLIED(3), respectively. Other information about the experiments and materials are shown in Supporting information.

Fig. 1 shows prepared PLIED electrodes' surface morphology, elements distribution, and phase composition. All of the PLIED PbO_2 electrodes show uniform porous morphology. As there is no exogenous template in the electro-deposition process, the porous morphology is caused by OER accompanied by PbO_2 anodic electrodeposition (Eqs. 4 and 5), which can be observed in the current responses during the process (Fig. S2 in Supporting information) [8,12]:

$$Pb^{2+} + H_2O \rightarrow PbO_2 + 4H^+ + 2e^- \quad (4)$$

$$2H_2O \rightarrow O_2 + 4H^+ + 4e^- \quad (5)$$

However, there are some apparent differences among the three porous PLIED electrodes. PLIED(1) electrode is formed by the rough particles with rocky-like morphology (Fig. 1a). PLIED(2) (Fig. 1b) and PLIED(3) (Fig. 1c) are formed by the smooth particles with cauliflower-like morphology, while the latter shows a larger aperture. The different particle shapes come from the different nucleation and growth process. PLIED(2) and PLIED(3) experience dramatic nucleation that weakens the particle growth and forms a more refined surface with small particles, which are proved by the higher current responses in Fig. S2 (Supporting information). Moreover, PLIED(2) shows the finest and most uniform pore, which may attribute to the better OER performance of SnO_2. Elements mappings show that lead and oxygen are evenly distributed on three PLIED electrodes (Figs. 1d–f). Combined with the average mass increasements in Fig. S3 (Supporting information), the atom ratios all approximate Pb:O = 1:2. As a result, it can be speculated that uniform porous PbO_2 coating was successfully deposited by rapid PLIED process.

XRD patterns of PLIED electrodes are displayed in Figs. 1g–i, which stand out the presence of β-PbO_2 on the surface of all three different substrates. Meanwhile, there are still some diffraction peaks belonging to substrates and their oxide in every XRD pattern, which may attribute to the short plating time resulting in the thinner coating. According to the phase identification results of XRD patterns, the proportion of β-PbO_2 is calculated and shown in Fig. S4 (Supporting information). The difference between PLIED(2) and PLIED(3) might explain the difference in mass increment with similar current responses. The average grain size and micro strain (ε) of surface PbO_2 are calculated and presented in Fig. S4 [13].

PLIED(2) shows the smallest grain size and the most significant micro strain, which could be attributed to the strong OER on SnO_2 substrate that influences the grain growth process and brings more

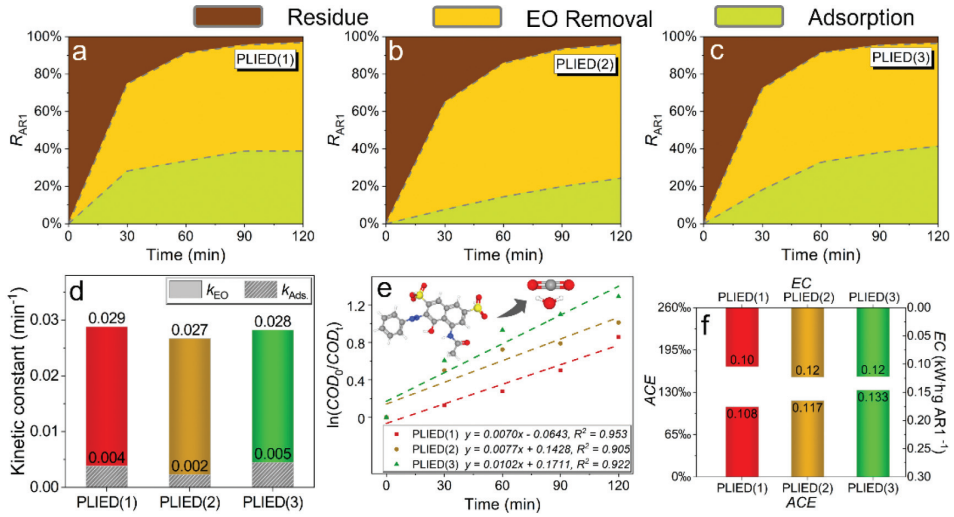

Fig. 2. Azophloxine degradation performance of PLIED electrodes, (a-c) acid red 1 removal by electrochemical oxidation and adsorption (100 mg/L AR1, 10 g/L Na_2SO_4, $j = 30$ mA/cm^2 for 120 min), (d) kinetic constants of electrochemical oxidation and adsorption, (e) COD removal kinetics, (f) average current efficiency and energy consumption during the degradation processes.

defects to PbO_2 lattice. The smallest grain size will bring more "active sites" to PLIED(2). PLIED(1) equipped with the minor micro strain will likely exhibit better stability in the process. It can be seen that for different substrate materials, due to their different physical and chemical properties, there may be differences in the corresponding optimal operation parameters of electrodeposition. The modification method starting from external circuit regulation and substrate selection is a more convenient substitution to various exogenous modifiers.

Fig. 2 exhibits the electrochemical degradation performance of AR1 by PLIED electrodes. As shown in Figs. 2a–c, all PLIED electrodes can complete decolorization of AR1, which is not much different from traditional PbO_2 electrodes fabricated by long-time electrodeposition [14,15]. Moreover, PLIED electrodes are shown adsorption capability to AR1. Considering the removal kinetics (Fig. 2d), the PLIED electrodes have similar removal rates. The subtle difference between PLIED(1) and PLIED(3) is likely caused by the different adsorption capabilities. Meanwhile, PLIED(3) shows the fastest COD removal rate (Fig. 2e), meaning there is fewer intermediates accumulation with PLIED(3). Therefore, PLIED(3) shows the highest current efficiency (Fig. 2f). The same trends of COD kinetics and average current efficiency also suggest the similar conductivities of three PLIED electrodes, coinciding with similar energy consumptions (Fig. 2f). PLIED electrodes display excellent electrochemical degradation performance to organics with higher concentration (100 mg/L), whatever the substrate's material is.

Considering the rising requirement for electrochemical wastewater treatment technology for emerging pollutants with low concentration, the degradation performance of PLIED electrodes to DCF-Na a typical non-steroidal anti-inflammatory drug also are evaluated (Fig. S5 in Supporting information) [16–18]. Figs. S5a–c shows that the R_{DCF} by PLIED electrodes all achieve 75% or above, especially PLIED(2) ($R_{DCF} = 93.4\%$), which is comparable with previous works about DCF degradation by other electrode materials or other advanced oxidation processes [19,20]. PLIED(2) displays similar adsorption capability both to DCF-Na (Fig. S5b) and AR1 (Fig. 2b), which also means that organics concentration varying on a particular scale will not influent the adsorption capability of PLIED(2). The reverse applies to PLIED(1) and PLIED(3). It implies the different adsorption mechanisms of the electrodes. The degradation performance of PLIED(1) and PLIED(3) closely depends upon pollutants concentration. As shown in Fig. S5e, PLIED(1) displays similar COD removal rate to PLIED(2), despite the removal rate of DCF being lower than that of PLIED(2), which is different from the situation of AR1 degradation. It may be caused by the different structures of the model pollutants. The current efficiency and energy consumption (Fig. S5f) show similar trends with kinetics in Figs. S5d and e, which agrees with the discussion on AR1 degradation. Hence, PLIED(1) and PLIED(2) are appreciated for the degradation of organics with a simple structure in low concentrations, while PLIED(3) is more suitable for complex organics in high concentrations.

To understand the degradation performance of the PLIED electrodes, the electrochemical activity of the electrodes is characterized. Fig. 3a shows the oxygen evolution potential (OEP) of PLIED electrodes from the cycle voltammetric curves shown in Fig. S6 (Supporting information). The lowest OEP and the highest current response (Fig. S6g) displayed by PLIED(3) explain its degradation performance. A high current response means a fast electrode reaction rate that makes the degradation process susceptible to mass transport situations under different concentrations. PLIED(2) shows high OEP and the highest hydroxyl radical productivity that entitle the electrode to excellent degradation performance, which is not affected by the property and concentration of pollutants to some extent. The highest OEP is exhibited by PLIED(1) because of the lowest hydroxyl radical productivity (Fig. 3b), which partly seems to conflict with its degradation performance. Cycle voltammetry (CV) curves (Fig. S6a) shown the stable presence of reversible redox couple, thus bringing the property of "active anode" into PLIED(1) to cover the shortage of hydroxyl radical [21]. Moreover, electrochemical porosity calculated from CV results (Figs. S6b, c, e, f, h, i) are shown in Fig. 3c, which suggests the electrochemical activity of the internal surface of the porous coating [22]. The high electrochemical porosity indicates the application potential of PLIED electrodes in a rising flow-through reaction system [23].

Stability is an essential issue for porous electrodes. Figs. 3d–f shows the AR1 removal and the cell potential during cycle degradation experiments of PLIED electrodes. The AR1 removal of three electrodes all steadily maintains on high-level, which suggests excellent electrochemical stability. PLIED(1) displays the slightest fluctuation of cell potential during degradation processes indicating favorable electrical stability, which may cause by a stable microstructure with the smallest micro strain. The cell potential fluctuation of PLIED(2) and PLIED(3) is slightly more significant than that of PLIED(1), keeping lower than 1 V. It could be seen that the three PLIED electrodes are all equipped with well electrical stabil-

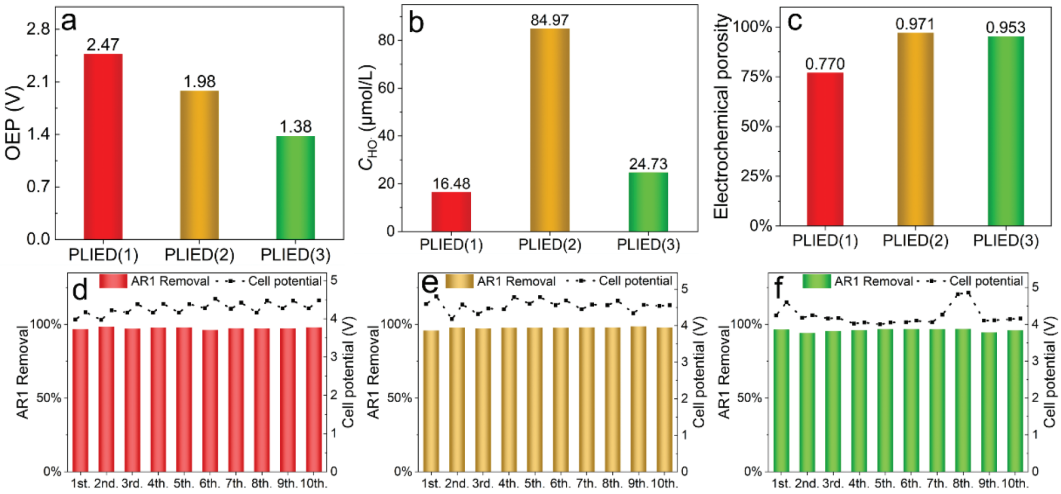

Fig. 3. Electrochemical activity and stability of PLIED electrodes, (a) oxygen evolution potential, (b) electrochemical porosity, (c) hydroxyl radical productivity (60 min galvanostatic electrolysis at 20 mA/cm^2 in dimethyl sulfoxide trapping solution), (d–f) electrochemical and electrical stability of PLIED(1), PLIED(2), and PLIED(3), respectively.

ity in organics degradation using. Considering the security issue of Pb for environmental application, the Pb(II) dissolution is evaluated at the different stages of the cycle degradations (Fig. S7 in Supporting information). The leakage of PLIED(2) and PLIED(3) is obviously slight than that of PLIED(1), suggesting that interlayer is helpful to improve the stability of porous electrode. After a few cycles, the Pb(II) dissolution decreased significantly. The activation and stabilization of PbO_2 electrode before use should be considered.

In this study, we realized the rapid preparation of uniform porous PbO_2 coatings in the form of external circuit potential linear increase. PbO_2 coatings with uniform pore size distribution on three substrates were obtained without adding a templating agent in 100 s, which greatly simplified the preparation process of porous PbO_2 coatings. Morphology and structure analysis shows that in addition to the introduction of exogenous modifier, external circuit regulation and physical and chemical properties of the substrate also have significant effects on the structure and properties of the coating. The performance evaluation of organic degradation suggests that three PLIED electrodes show excellent electrochemical conversion and mineralization capability to specific dye and pharmaceutical with different concentrations. The electrochemical activity tests proved that PLIED electrodes' healthy electrochemical oxidation properties derive from different mechanisms. The electrochemical stability of PLIED electrodes with different substrates is similar, but the electrical stability varies with the substrate materials. According the comparison results in Tables S2 and S3 (Supporting information), the PLIED electrodes show high OEP and slight lead dissolution, which suggests the comparable catalytic activity and safety with modified PbO_2 electrodes. As a unique advantage of electrocatalytic reaction, the regulatory role of external circuits may deserve more attention. Moreover, the adsorption capability of porous electrodes needs further investigation.

Declaration of competing interest

The authors declare that they have no known competing financial interests or personal relationships that could have appeared to influence the work reported in this paper.

Acknowledgments

The authors gratefully acknowledge the financial supports from the National Natural Science Foundation of China (No. 52270078), the Natural Science Basic Research Plan in Shaanxi Province of China (No. 2021JM-012), the Welfare Technology Research Plan of Zhejiang Province (No. LZY21E080003), and the Fundamental Research Funds for the Central Universities (No. xjh012020037).

Supplementary materials

Supplementary material associated with this article can be found, in the online version, at doi:10.1016/j.cclet.2022.108030.

References

[1] Q. Zhou, X. Zhou, R. Zheng, Z. Liu, J. Wang, Sci. Total Environ. 806 (2022) 150088.
[2] B.H. Yu, R.D. Xu, X.B. Wang, W.B. Wang, S.Y. Feng, Renew. Energy 159 (2020) 885–892.
[3] X. Fu, Y. Han, H. Xu, Z. Su, L. Liu, J. Hazard. Mater. 422 (2022) 126890.
[4] D. Shao, Z. Wang, C. Zhang, et al., Chin. Chem. Lett. 33 (2022) 1288–1292.
[5] H. Guo, W. Hu, Z. Xu, et al., Process Saf. Environ. Prot. 164 (2022) 189–207.
[6] H. Guo, Z.C. Xu, D. Qiao, et al., Chemosphere 261 (10) (2020) 128157.
[7] M. Xu, Y.L. Mao, W.L. Song, et al., J. Electroanal. Chem. 823 (2018) 193–202.
[8] N. Comisso, S. Cattarin, P. Guerriero, et al., Electrochem. Commun. 60 (2015) 144–147.
[9] Y.W. Yao, C.J. Huang, Y. Yang, M.Y. Li, B.L. Ren, Chem. Eng. J. 350 (2018) 960–970.
[10] X. Li, D. Pletcher, F.C. Walsh, Chem. Soc. Rev. 40 (2011) 3879–3894.
[11] H. Guo, Z. Xu, D. Qiao, et al., Water Environ. Res. 93 (2021) 42–50.
[12] Y.W. Yao, X. Chen, N.C. Yu, H.S. Dong, H.R. Wang, J. Electrochem. Soc. 164 (2017) E48–E52.
[13] Y. Zhou, Z. Li, C. Hao, et al., Electrochim. Acta 333 (2020) 135535.
[14] M. Yuan, N.M. Salman, H. Guo, et al., Catalysts 9 (2019) 875.
[15] J. Lei, Z. Xu, H. Xu, et al., J. Environ. Chem. Eng. 8 (2020) 103773.
[16] Y. Ren, W. Zheng, X. Duan, N. Goswami, Y. Liu, Environ. Funct. Mater. 1 (2022) 10–20.
[17] H. Li, S. Sun, H. Ji, W. Liu, Z. Shen, Appl. Catal. B: Environ. 272 (2020) 118966.
[18] Q. Liu, H. Li, H. Zhang, Z. Shen, H. Ji, Chin. Chem. Lett. 33 (2022) 4756–4760.
[19] F. Han, X. Ye, Q. Chen, H. Long, Y. Rao, Sep. Purif. Technol. 232 (2020) 115967.
[20] H. Guo, Z. Xu, D. Wang, et al., Chemosphere 286 (2022) 131580.
[21] D. Guo, S. You, F. Li, Y. Liu, Chin. Chem. Lett. 33 (2022) 1–10.
[22] H. Lin, J.F. Niu, S.T. Liang, et al., Chem. Eng. J. 354 (2018) 1058–1067.
[23] D. Guo, Y. Liu, H. Ji, et al., Environ. Sci. Technol. 55 (2021) 4045–4053.